Cyclic Hardening Property and Low Cycle Fatigue Behavior of Aluminum Alloys†

Kohsuke HORIKAWA*, Sang-Moung CHO**

Abstract

Fatigue crack initiation life of a structure may be determined by local mechanical conditions such as local stress and/or strain, and by local material properties. The present work is intended to predict fatigue crack initiation life of a structure by means of local fatigue concept and fatigue behaviors of smooth specimens. 4 kinds of Al alloys were tested to investigate the cyclic hardening properties and failure lives by strain control fatigue tests. Load control fatigue tests were performed to observe crack initiation behaviors in notched specimens (K_t = 2.3). The effect of cyclic hardening properties on local bahaviors in notch tip was also discussed.

KEY WORDS: (Notch) (Fatigue Crack Initiation) (Low Cycle Fatigue) (Cyclic Hardening Property)

1. Introduction

Various stress concentrated areas (stress concentrations) or notches may be formed in structures at the stage of design and manufacturing.

In the stress concentrations, high stresses occur, and mechanical properties of materials can be also changed.

Generally, in the case of the structures loaded cyclically, fatigue cracks are initiated in these stress concentrations.

It is said that fatigue life of structural components is composed of two parts: crack initiation and crack propagation life. The latter for long cracks can be evaluated by application of fracture mechanics,[1] though that is not simple for components of complicate structures. But, for crack initiation and propagation life of short cracks at early stage in notch tip, it is very difficult to estimate the lives separately because the shape of notches, stress level and material properties affect them.[2-4]

Accordingly, it is usually considered that crack initiation life includes even propagation life of short cracks.[4-7]

On the other hand, crack initiation life of a structure may be determined by local mechanical quantity such as local stress and/or strain, and by local materials or characteristic of the material properties change under cyclic load, by so-called local fatigue behavior. Therefore, it seems that the local fatigue behavior should be, especially over the range of low and medium cycle fatigue, considered in the design of materials as well as fatigue design and manufacturing of structures subjected to cyclic load.

It is worthwhile to mention that, if local mechanical quantity of a component with notch and mechanical quantity of a smooth specimen are the same, crack initiation life of the former is nearly equal to failure life of the latter.[8-10] The present work is based on this concept. Although there are some problems on the concept, that has been used until now because of the simplicity of the application procedure. The cyclic stress-strain curves and failure life curves of smooth specimens must be obtained basically. And if local mechanical quantity of a notched component is given, crack initiation life of it can be estimated immediately.

It is the objective of this study to investigate the cyclic hardening properties of 4 kinds of Al alloys, to compare the failure life of smooth specimens with crack initiation life of notched specimens, and to examine local strain amplitude ϵ_a[6),8)] and fatigue damage parameter P_{SWT}[9-10)] as local mechanical quantity in notched specimens.

In practice, smooth specimens were tested to obtain cyclic stress-strain curves by the incremental step test, and to get failure life curves by the axial strain control ($R_\epsilon = -1$). For notched specimens, fatigue tests by axial load control ($R_\sigma = -1$) were carried out to investigate crack initiation behavior.

The effect of cyclic hardening property on local

† Received on Nov. 11, 1985

* Associate Professor
** Graduate Student

Transactions of JWRI is published by Welding Research Institute of Osaka University, Ibaraki, Osaka 567, Japan

mechanical quantity in notch tip was discussed.

2. Materials and Experimental Procedure

The specimens used in the experiments were plates. The kinds of materials were A5083-0 and A7N01-T4 which were used mostly in welded structures, and A7178-T6 and A7016-T6 which had very high strength. Chemical composition of material is given in Table 1.

According to ASTM E606 (1983), the smooth specimens which were used in cyclic load tests and low cycle fatigue tests by axial strain control were shaped as shown in Fig. 1 (a). The notched specimens tested by axial load control had a center hole with 2.5 mm root radius, and also two small grooves with 1.0 mm root radius in both sides of it as shown in Fig. 1 (b). These grooves were needed to measure the range of notch displacement by ring type clip gage.

Elastic stress concentration factor K_t of the notch was 2.3 by elastic FEM. Elastic FEM analysis was carried out under plane stress condition and minimum size of triangular element was 0.3 mm that was about 0.1 R1 (R1 is root radius of the center hole).

Cyclic load tests of smooth specimens were performed by clip gage with gage length 10.0 mm. The cyclic stress-strain curves were determined by means of incremental step test in which maximum value of total strain amplitude were 1.4% and strain rate was 0.004/sec.

To obtain failure life curves of the smooth specimens, low cycle fatigue tests were conducted also by the axial strain control ($R_\epsilon = -1$) with strain rate 0.003–0.005/sec.

To diminish the influence of dynamic creep strain, fully-reversed axial load ($R_\sigma = -1$) were applied to the notched specimens with load speed 0.3–2.0 Hz.

Table 1 Chemical compositions of materials (wt%)

Materials	Si	Fe	Cu	Mn	Mg	Cr	Zn	Ti	Zr
A5083-0	0.13	0.21	0.02	0.64	4.51	0.13	0.01	0.01	–
A7N01-T4	0.05	0.13	0.09	0.5	1.2	0.23	4.79	0.02	0.1
A7016-T6#	0.07	0.18	0.6	0.05	1.5	0.01	5.3	0.01	0.12
A7178-T6#	0.07	0.18	1.8	0.3	2.6	0.2	6.5	0.01	–

#: Aging treatment (120°C × 24 Hr)

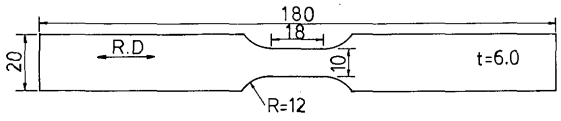

(a) Configuration of smooth specimens

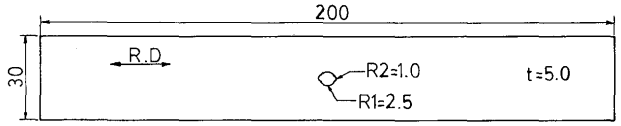

(b) Configuration of notched specimens

Fig. 1 Configuration of specimens (unit: mm)

All tests were performed on servo-hydraulic system (SHIMAZU, dynamic capacity 5.0 TON), and at ambient room temperature.

3. Results and Discussion

3.1 Cyclic stress-strain response

Fig. 2 shows monotonic and cyclic stress-strain curves for all tested materials. In Fig. 2, monotonic and cyclic behavior are indicated by solid and dashed lines respectively. In each cyclic stress-strain curve, the stress amplitude σ_a versus the corresponding strain amplitude ϵ_a was obtained at half-life of failure blocks.

It is clear that A5083-0 and A7N01-T4 show remarkable cyclic hardening, but A7178-T6 and A7016-T6 do not reveal obvious cyclic hardening or softening.

The response of materials as Fig. 2 can be written as following equation (1) and (2)

$$\text{Monotonic response:} \quad \epsilon = \frac{\sigma}{E} + \left(\frac{\sigma}{C}\right)^{\frac{1}{n}} \qquad (1)$$

$$\text{Cyclic response:} \quad \epsilon_a = \frac{\sigma_a}{E} + \left(\frac{\sigma_a}{C'}\right)^{\frac{1}{n'}} \qquad (2)$$

where $\epsilon_a = \frac{\Delta\epsilon}{2}$, $\sigma_a = \frac{\Delta\sigma}{2}$

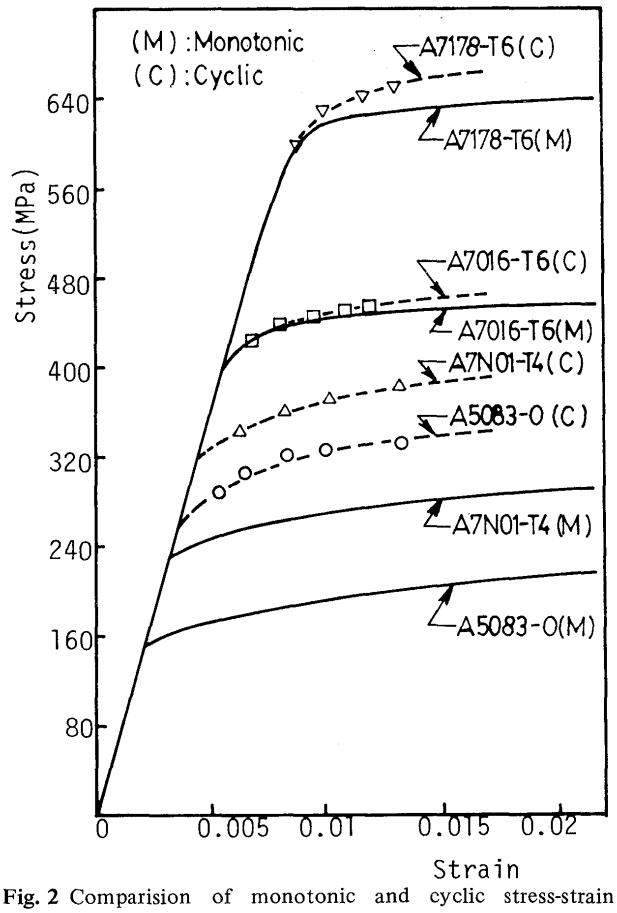

Fig. 2 Comparision of monotonic and cyclic stress-strain behavior.

As shown Table 2, material constants were determined by least square method, their valid range was as follows:

Monotonic response: $\epsilon \leqslant 3.5 \sim 8.0\%$

Cyclic response: $\epsilon_a \leqslant 1.4\%$,

Table 2 Results of monotonic and cyclic tests

Materials	Monotonic test					Cyclic test		
	E (GPa)	σ_Y (MPa)	σ_u (MPa)	C	n	C'	n'	$\sigma_{YC}^{\#}$ (MPa)
A5083-0	68.6	172.0	320.5	514.5	0.194	481.9	0.073	305.8
A7N01-T4	71.6	254.0	399.8	466.0	0.104	547.3	0.072	350.1
A7016-T6	71.6	434.7	494.0	558.8	0.04	555.3	0.038	439.3
A7178-T6	71.6	618.6	665.9	761.1	0.032	851.1	0.045	642.3

#: $\sigma_{YC} = C' (0.002)^{n'}$

Table 2 shows that, in the same manner of steel[11], strain hardening exponent n in monotonic response varies considerably with the kind of material, but cyclic hardening exponent n' in cyclic response does not vary so much.

Examining the relation of yield ratio YR ($= \sigma_Y/\sigma_u$) and cyclic hardening properties of materials, A5083-0 and A7N01-T4 with YR of 0.54 and 0.64 were hardened significantly by cyclic load, but A7178-T6 and A7016-T6 with YR of 0.93 and 0.88 revealed nearly stable behavior.

Commonly, in metallic material which has not Lüders strain, it shows cyclic hardening if YR of it is below 0.71, but it does cyclic softening if YR of it is above 0.84, between two values it does stable behavior[12]. It was also confirmed through the present experiment that yield ratio YR, which can be obtained by monotonic test, may be an index by which cyclic hardening property of material can be judged.

3.2 Low cycle fatigue of smooth specimens by strain control

Deformation of material in plastic zone is constrained by elastic material around it when plastic zone at notch tip is small. For that reason, it is generally known that the behavior of the material in the plastic zone becomes nearly strain control fatigue even though load control fatigue.[3),13)] Based on this concept, fatigue test by strain control is carried out for smooth specimen when crack initiation life of notched specimen is compared with failure life of smooth specimen.

Fig. 3 shows hysterisis loops from 1st to 8th cycle of A5083-0 when total strain amplitude ϵ_a of 0.6% was applied with constant value. Seeing that stress amplitude becomes higher in spite of constant amplitude of total strain, cyclic hardening is remarkable in this case.

The stress amplitude is changed violently at early stage, but becomes stable gradually. In this way, stable condition may be accomplished until half of failure life as shown in Fig. 4.

However, if plastic strain does not occur from the first

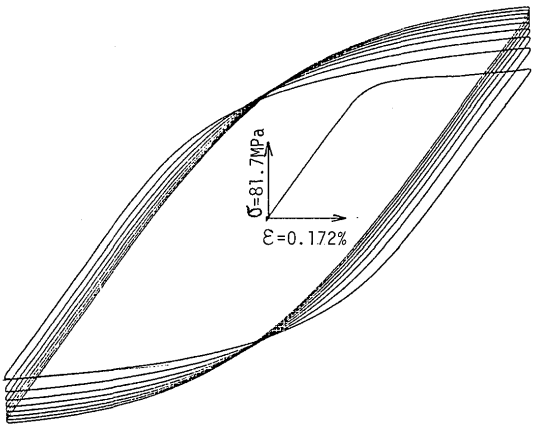

Fig. 3 Hysterisis loops from 1st to 8th cycle at ϵ_a = 0.6% (A5083-0)

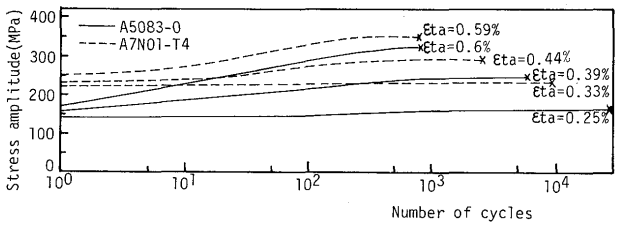

Fig. 4 Change of stress amplitude versus number of cycles in strain control fatigue test.

cycle, as $\epsilon_a = 0.25\%$ of A5083-0 and $\epsilon_a = 0.33\%$ of A7N01-T4 in Fig. 4, stress amplitude hardly changes. It is well known that cyclic hardening or softening needs plastic strain which is applied reversibly.[12)] A part of the concept was validated through the present work.

Fig. 5 shows the relation of total strain amplitude ϵ_a and failure life N_f for smooth specimens by fully-reversed strain control.

In Fig. 5, there is little variation on fatigue strength of materials in lower cycle range as 10^3 cycle. In higher cycle range as 10^5 cycle, fatigue strength varies with materials, in particular, is affected by monotonic strength. As the result, at 10^5 cycle failure life, fatigue strength becomes higher in following order: A5083-0, A7N01-T4, A7016-T6, A7178-T6.

Fig. 6 was plotted by fatigue damage parameter P_{SWT} ($= \sqrt{\sigma_{max} \cdot \epsilon_a \cdot E}$)[10)] instead of total strain amplitude ϵ_a in Fig. 5. The parameter P_{SWT} is accepted that the effect of mean stress and residual stress can be introduced simply by means of maximum stress σ_{max}.

In lower cycle range as 10^3 cycle, variation of failure

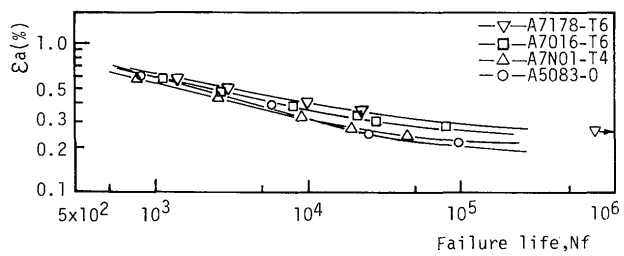

Fig. 5 Total strain amplitude ϵ_a versus fatigue failure life N_f in smooth specimens.

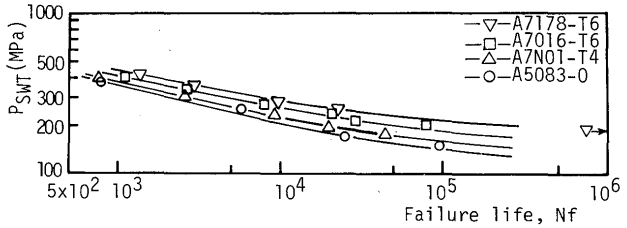

Fig. 6 Fatigue damage parameter P_{SWT} versus fatigue life N_f in smooth specimens.

life curves becomes larger in Fig. 6 than in Fig. 5, because σ_{max}, here $\sigma_{max} = \sigma_a$, varies with cyclic stress-strain relation of each material.

On the other hand, in the case of A7016-T6 and A7178-T6 (both aged 24 Hr at 120°C), macro-plastic strain could be hardly measured even if for the shortest failure life of each material. This can mean that slip zone is very localized in precipitate-free zone (PFZ) which may be formed prior to or during cycling, and then micro-cracks may initiate in the slip zone.[12),14)]

3.3 Fatigue crack initiation of notched specimens

Fig. 7 gives the relation between the range of notch displacement (ΔND) and the number of cycles in A5083-0. Here, crack initiation life N_c1 was defined by the cycle number when the ΔND began to increase from stable condition. And crack initiation life N_c2 was defined by the cycle number when a crack at notch root grew into 0.5 mm.

Keeping constant cyclic load in A5083-0 as Fig. 7, the ΔND decreases if material at notch root yields from the first cycle. In practice, total strain range at notch root decreases due to considerable cyclic hardening.

It can be said that the material at notch tip is deformed under fully-reversed strain control ($R_\epsilon = -1$) when stable condition is built up at near crack initiation life N_c1.

In Fig. 8, (a) shows the relation of nominal stress amplitude S_a and crack initiation life N_c1, (b) shows the relation of nominal stress amplitude S_a and crack initiation life N_c2. The bold lines mean the data on smooth specimens. From Fig. 8 (a), it is obvious that fatigue notch factor K_f is smaller than $K_t = 2.3$. In practice, the mean value of K_f is about 1.7 in all notched specimens.

Fig. 9 shows the relation of crack initiation life ratio N_cR (= N_c/N_f) and failure life N_f. Here, (a), (b) give the relation of N_c1R and N_f, the relation of N_c2R and N_f respectively. N_cR may varies with, first of all, configuration of specimen, but that is the same in the present work. Besides, we could confirm that N_cR could be changed also by the kind of material and stress level or failure life. In Fig. 9, the larger N_f becomes, as a whole, the larger N_cR becomes. That is to say, the contribution of crack initiation life to failure life is larger under the low stress than under the high. Moreover, the N_cR of A7178-T6 is, in the present study, the largest, whereas the N_cR of A7N01-T4 is the smallest. Difference between the tendency of N_c1R and N_c2R, though that is not striking, might result from initiation and propagation properties of short cracks at notch root. Going into details, there were the cases that a dominant crack initiated in a section and then propagated into a long one, and that several cracks initiated at early

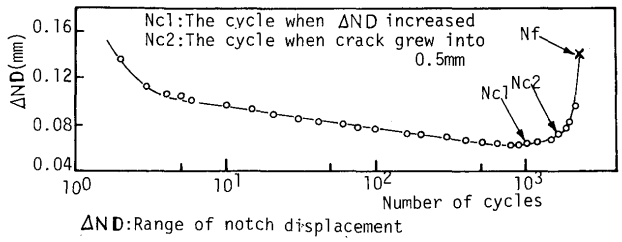

Fig. 7 Change of ΔND versus number of cycles (A5083-0)

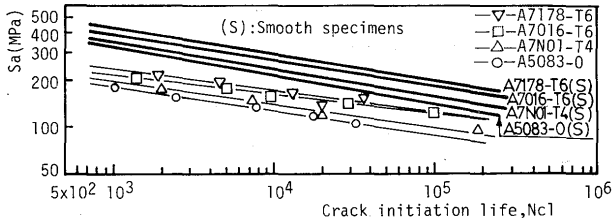

(a) Nominal stress amplitude S_a vs. crack initiation life N_c1

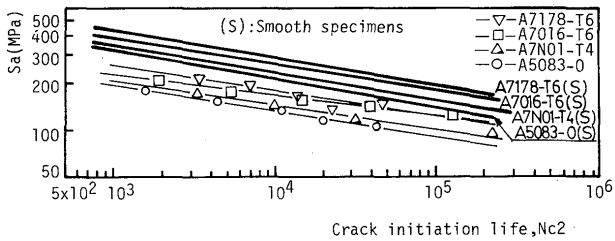

(b) Nominal stress amplitude S_a vs. crack initiation life $Nc2$

Fig. 8 Relation of nominal stress S_a and crack initiation life N_c1 or N_c2 of notched specimens.

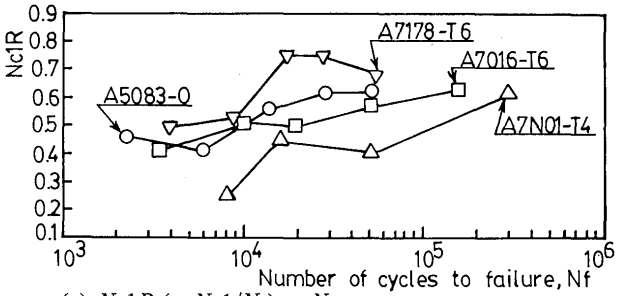

(a) N_c1R ($= N_c1/N_f$) vs. N_f

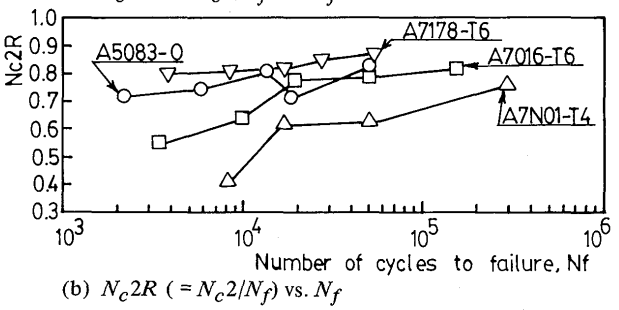

(b) N_c2R ($= N_c2/N_f$) vs. N_f

Fig. 9 The ratio of crack initiation life N_c1 or N_c2 to failure life N_f in notched specimens.

stage, then a dominant crack grew into a long one. For example, A7178-T6 could be related to the former, A7N01-T4 could the latter.

Namely, initiation and propagation properties of short cracks at notch root were varied by material and stress level.

Fig. 10 denotes the relation between local strain amplitude ϵ_a and crack initiation life N_c1 in notched specimens of A5083-0. For estimation of local strain amplitude, the two methods of Neuber's rule[15] and numerical analysis[16] were adopted, and two kinds of material constants that were obtained by monotonic and cyclic tests were used for each method. The bold line in Fig. 10 indicates the behaviors of smooth specimens.

Here, in the case of Neuber's rule, from the relation of

$$K_t = K_\sigma \cdot K_\epsilon \tag{3}$$

and

$$\left(\frac{\sigma}{\sigma_Y}\right) = \left(\frac{\epsilon}{\epsilon_Y}\right)^{n_2} \tag{4}$$

for the stress-strain relation of materials, putting $K_f = K_t$ in Eq.(3), substituting stress and strain amplitude for stress and strain in Eq.(4), local strain amplitude ϵ_a can be written by

$$\begin{aligned} \epsilon_a &= K_f \cdot e_a && K_f \cdot e_a \leqslant \epsilon_Y \\ \epsilon_a &= K_f e_a \left(K_f \frac{S_a}{\sigma_Y}\right)^{-(n'_2-1)/(n'_2+1)} && K_f \cdot e_a > \epsilon_Y \end{aligned} \tag{5}$$

where,

K_σ, K_ϵ: stress and strain concentration factor.

σ_Y, ϵ_Y: yield stress and strain.

S_a, e_a: nominal stress and strain amplitude.

In the case of numerical analysis, the master curves in Reference [16] were applied. Both the two kinds of methods were proposed to denote the monotonic behaviors of materials. However, in this paper they were applied to fatigue of notched specimens.

In Fig. 10, fatigue crack initiation curves are changed exceedingly by the estimation method of local strain and by used material constants.

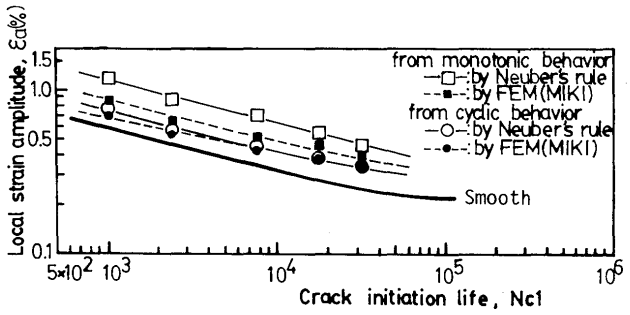

Fig. 10 Relation of local strain amplitude and crack initiation life by several methods (A5083-0)

Comparing notched specimens with smooth ones, as expected, crack initiation curves of notched specimens were closer to failure curve of smooth ones when local strain amplitude was calculated by material constants through cyclic tests than monotonic tests.

On the other hand, the reason on difference between the behavior of Neuber's rule and numerical analysis will be discussed in the next section. But Neuber's rule rather than numerical method was used in Fig. 11 on account of the simplicity of application.

Making use of material constants by cyclic tests and Neuber's rule on all notched specimens, the relations of local strain amplitude ϵ_a and crack initiation life N_c1 were given as Fig. 11. The bold lines indicate the data on smooth specimens. As a whole, curves on notched specimens were located in high strength region in comparision with smooth ones. This trend would be caused by overestimation of K_f, which put to use K_t of 2.3 directly.

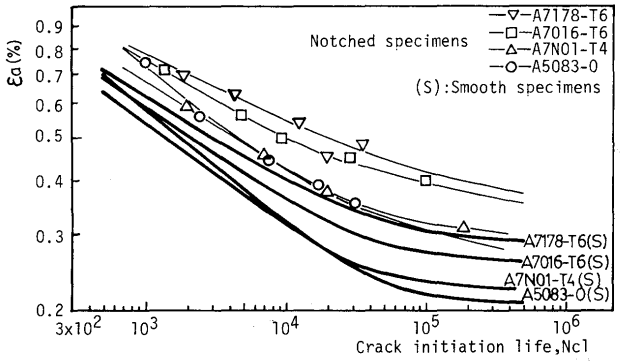

Fig. 11 Local strain amplitude ϵ_a versus crack initiation life N_c1 in notched specimens.

Whereas, crack initiation life curves were closer to failure curves of smooth specimens, in case of A5083-0 in which considerable plastic strain existed during fatigue tests than in case of A7178-T6 and A7016-T6 in which usually did not exist plastic strain during the tests.

Fig. 12 shows the relation of fatigue damage parameter P_{SWT} and crack initiation life N_c1. Putting $K_f = K_t$, from Eq.(3) P_{SWT} can be written by

$$P_{SWT} = K_f \cdot S_a = \sqrt{\sigma_{\max} \cdot \epsilon_a \cdot E} \tag{6}$$

In Fig. 12, there is a similar tendency to Fig. 11. But A5083-0 which took largest strain during the fatigue tests, exhibits a different tendency to the result of evaluation by local strain. If plastic strain does not occur, it seems that the difference between the results by ϵ_a and P_{SWT} scarecely appears, because the present tests are fully-reversed fatigue.

Consequently, in the case of fully-reversed fatigue, if tip of notch deformes under elastic condition, two parameters of ϵ_a and P_{SWT} result in nearly the same. But if tip of notch takes plastic behavior, the results of evaluation

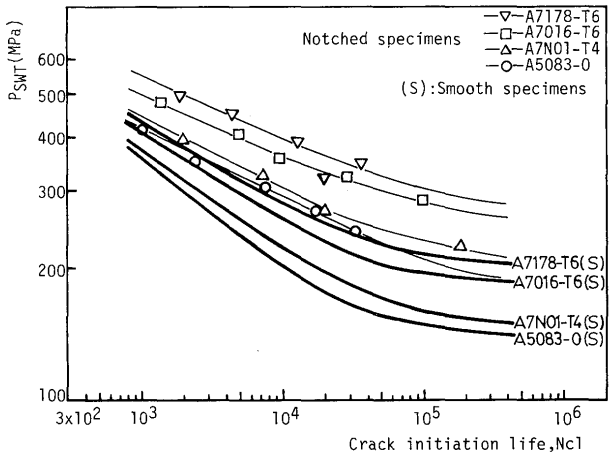

Fig. 12 Fatigue damage parameter P_{SWT} versus crack initiation life N_c1 in notched specimens.

by ϵ_a rather than P_{SWT} are closer to the behavior of smooth specimens.

3.4 Discussion

If load and shape of a component were offered, local mechanical quantity can be obtained. Then crack initiation life of the component can be predicted by the data of smooth specimens with the same condition. To do this prediction, it is necessary that mechanical behavior of material at the notch tip (local material) should be examined exactly.

In this section, the influence of cyclic hardening property upon mechanical behavior of local material (local behavior) will be discussed.

If local stress exceeds yield strength, local behavior is very complicated. Fig. 13 gives the local behavior in notched specimen of A5083-0. The solid lines indicate the behavior by Neuber's rule. The dashed lines mean the results of numerical analysis. As stated in the prior section, these two methods had been proposed for monotonic behavior of notched specimen. But the two methods,

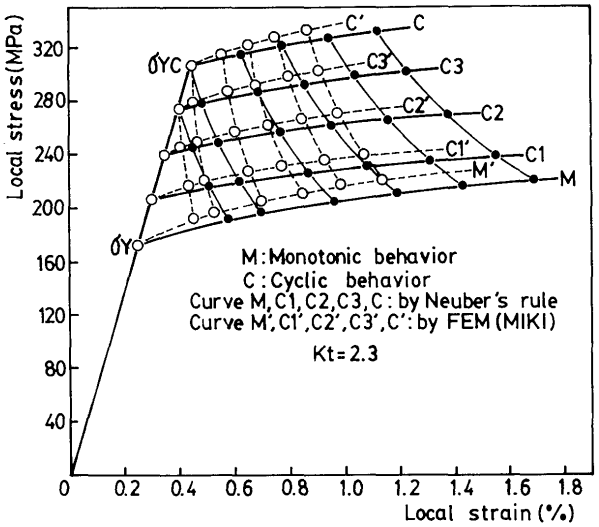

Fig. 13 Change of local stress-strain relation by cyclic hardening property (A5083-0)

here, are applied to consider the influence of cyclic hardening property upon local behavior in fatigue.

Curve M, M' show monotonic behavior, curve C, C' stable cyclic behavior, and curve C_n, C_n' transitional behavior until stable state.

It is assumed that local material takes, at first monotonic behavior M or M' and transitional behavior C_n or C_n', at last stable behavior C or C' (see Fig. 7). Material constant σ_{YC} and n_2' used in stable behavior C or C' are the values obtained by cyclic tests under fully-reversed strain control. On the transitional behavior C_n or C_n', it is supposed that only σ_{YC} undergoes a change, n_2' takes the same value to the stable behavior.

By J-integral or numerical analysis on monotonic behavior, Neuber's rule of Eq.(3) can be given by[16]

$$mK_t = K_\sigma \cdot K_\epsilon \tag{7}$$

In Eq.(7), the value of m becomes 0.5 to 1.0. As the prior section, applying Eq.(7) to fatigue, putting $K_f = K_t$, presuming that nominal stress amplitude S_a is below yield strength, Eq.(7) can be written by

$$mK_f \cdot S_a = \sqrt{\sigma_a \cdot \epsilon_a \cdot E} \tag{8}$$

In Eq.(8), if m is equal to 1.0, the value of $K_f \cdot S_a$ becomes P_{SWT}. On that account, local mechanical quantity P_{SWT} is not affected by cyclic hardening property of local material. Namely, in Fig. 13, even though a point on the monotonic behavior M transfers to on the curve C1, C2, C3, at last settles down on the stable cyclic behavior C, the value of $\sigma_a \cdot \epsilon_a$ is kept up constant.

Considering local strain amplitude ϵ_a in Eq.(8), ϵ_a can be equated by

$$\epsilon_a = \frac{K_f^2 \cdot S_n^2}{E} \frac{1}{\sigma_a} \tag{9}$$

Because $K_f \cdot S_a / E$ is constant, the relation of ϵ_a and σ_a result in hyperbolic curves as solid lines from M to C in Fig. 13.

Discribing the case that m takes 0.5 to 1.0, m approaches 0.5 when local behavior is plastic, whereas m becomes 1.0 when local behavior is elastic. Therefore, the left term in Eq.(8) becomes larger if local material is hardened by cyclic load, but smaller if softened.

On the other side, from Eq.(8), local strain amplitude ϵ_a can be given by

$$\epsilon_a = \frac{K_f^2 \cdot S_a^2}{E} \frac{m^2}{\sigma_a} \tag{10}$$

where, m is a function of $\dfrac{K_f \cdot S_a}{\sigma_{YC}}$ and n_2'

Even if ϵ_a is a function of m^2/σ_a, the relation of ϵ_a and σ_a may result in shape of hyperbolic curves as the dashed lines from M' to C' in Fig. 13.

Examining $\sigma_a \cdot \epsilon_a$ by Neuber's rule and numerical analysis, $\sigma_a \cdot \epsilon_a$ by Nueber's rule does not vary with cyclic hardening property of material, but by the other does vary with it.

Moreover, considering the variation of only ϵ_a by Nueber's rule and numerical analysis, ϵ_a by Nueber's rule is proportional to $1/\sigma_a$, but by the other m^2/σ_a. For that reason, even if local material is hardened or softened by cyclic load, the variation of ϵ_a by Nueber's rule is always larger than by the other.

In fact, Bauchinger effect has not considered in Eq.(8). This problem may be needed to investigate in detail.

4. Conclusion

For 4 kinds of medium and high strength Al alloys, the cyclic hardening properties were investigated. And strain control fatigue tests were performed for smooth specimens, load control fatigue tests were carried out to observe crack initiation behavior in notched specimens. The influence of cyclic hardening property on mechanical behavior of local material in notched specimen was discussed.

The following conclusion may be drawn:

1) A5083-0 and A7N01-T4 exhibited remarkable cyclic hardening, but A7178-T6 and A7016-T6 did stable behavior.
2) It was confirmed that yield ratio YR $(= \sigma_Y/\sigma_u)$ may be an index by which cyclic hardening property can be judged.
3) In the relation of total strain amplitude ϵ_a and failure life N_f for smooth specimens by strain control fatigue, there was little variation on fatigue strength of in lower cycle range as 10^3, but in higher cycle range as 10^5, fatigue strength varied with materials, namely, was affected by monotonic strength.
4) Fatigue crack initiation ratio N_cR $(= N_c/N_f)$ was altered by both kind of material and stress level even though the shape of specimen was the same.
5) In the case of load control without mean stress, if local behavior at notch root was elastic, two parameters of ϵ_a and P_{SWT} resulted in nearly the same, but if local behavior was plastic, the results of evaluation by ϵ_a than by P_{SWT} was closer to the behavior of smooth specimens.
6) P_{SWT} by Nueber's rule in notched specimen did not vary with cyclic hardening property, but by numerical method did vary with it. Moreover, even though local material at notch root was hardened or softened by cyclic load, the variation of ϵ_a by Nueber's rule was always larger than by numerical analysis.

Reference

1) K. Horikawa, A. Sakakibara, T. Mori: Effect of Residual Stresses on Threshold Value for Fatigue Crack Propagation, Trans. of JWRI. Vol. 12 (1983), No. 2, pp 295–302.
2) T.R. Brussat: Estimating Initiation Times of Secondary Fatigue Cracks in Damage Tolerance Analysis, Fatigue of Engineering Materials and Structures Vol. 6 (1983), No. 3, pp 281–292.
3) B.N. Leis: Displacement Controlled Fatigue Crack Growth in Inelastic Notch Fields, Engineering Fracture Mechanics Vol. 22 (1985), No. 2, pp 279–293.
4) D.F. Socie, N.E. Dowling, P. Kurath: Fatigue Life Estimation of Notched Members, ASTM STP 833 (1984), pp 284–299.
5) D. Rhodes: Limit to the Applicability of LEFM in Notch Fatigue, Engineering Fracture Mechanics Vol. 19 (1984), No. 5, pp 911–918.
6) K. Iida: Application of the Hot Spot Strain Concept to Fatigue Life Prediction, Welding in the World Vol. 22 (1984), No. 9/10, pp 222–246.
7) M. Nihei, P. Heuler, C. Boller, T. Seeger: Fatigue Life Prediction by Use of Damage Parameter, J. of the Society of Naval Architecs of Japan Vol. 156 (1984), pp 469–477, (in Japanese).
8) S.S. Manson: Fatigue: A Complex Subject-some Simple Approximations, Experimental Mechanics (July 1965), pp 193–226.
9) B.M. Wundt: Effect of Notches on Low-cycle Fatigue, ASTM STP 490 (1972), pp 11–13.
10) K.N. Smith, T.H. Watson, T.H. Topper: A Stress-strain Function for the Fatigue of Metals, J. of Materials 5 (1970), No. 4, pp 767–768.
11) S. Nishijima, et al.: Axial Load Fatigue Properties of JIS Machine Structural Carbon Steels, Cr and Cr-Mo Steels. Trans. JSME (A) Vol. 46 (1980), No. 412, pp 1314–1328, (in Japanese).
12) M. Klesnil, P. Lukas: Fatigue of Metallic Materials, Elsevier, Czechoslovakia (1980), pp 12–56.
13) S.T. Rolfe, J.M. Barsom: Fracture and Fatigue Control in Structures, Prentice-Hall, New Jersey, U.S.A. (1977), pp 208–231.
14) A. Gysler, J. Lindigkeit, G. Lutjering: Correlation between Microstructure and Fatigue Fracture, 5th Int. Conf. on the Strength of Metals and Alloys, West German (1979), pp 1113–1118.
15) H. Neuber: Theory of Stress Concentration for Shear-strained Prismatical Bodies With Arbitrary Nonlinear Stress-Strain Law, J. Applied Mech. ASME. (Dec. 1961), pp 544–550.
16) N. Miki: Stress Concentration in the Elastic-plastic Region, Materials, Vol. 33 (1984), No. 373, pp 1–9. (in Japanese).